Seasonal iron depletion in temperate shelf seas

Antony J. Birchill[1], Angela Milne[1], E. Malcolm S. Woodward[2], Carolyn Harris[2], Amber Annett[3], Dagmara Rusiecka[4,5], Eric P. Achterberg[4,5], Martha Gledhill[4.5], Simon J. Ussher[1], Paul J. Worsfold[1], Walter Geibert[6], Maeve C. Lohan[5]

[1] School of Geography, Earth and Environmental Sciences, University of Plymouth, Drake Circus, Plymouth, PL4 8AA, United Kingdom.
[2] Plymouth Marine Laboratory, Prospect Place, The Hoe, Plymouth, PL1 3DH, United Kingdom.
[3] School of Geoscience, University of Edinburgh, Grant Institute, The King's Buildings, West Mains Road, Edinburgh, EH9 3FE, United Kingdom.
[4] GEOMAR Helmholtz Centre for Ocean Research, 24148 Kiel, Germany.
[5] Ocean and Earth Science, University of Southampton, National Oceanography Centre, Southampton, SO14 3ZH, United Kingdom.
[6] Alfred Wegener Institute, Am Handelshafen 12, Bremerhaven, Germany

Corresponding author: Antony J. Birchill (antony.birchill@plymouth.ac.uk)

Key Words

dissolved iron; colloidal iron; particulate iron; nitrate; Celtic Sea; shelf sea biogeochemistry

Key Points

1. Preferential uptake of soluble iron during the phytoplankton spring bloom implies that it is initially more bioavailable than colloidal iron

2. Potentially growth limiting concentrations of bioavailable iron during summer in the Celtic Sea as a result of seasonal stratification

3. Organic matter remineralisation drives a seasonal increase in dissolved iron independent of particulate iron cycling

This article has been accepted for publication and undergone full peer review but has not been through the copyediting, typesetting, pagination and proofreading process which may lead to differences between this version and the Version of Record. Please cite this article as doi: 10.1002/2017GL073881

Abstract

Our study followed the seasonal cycling of soluble (SFe), colloidal (CFe), dissolved (DFe), total dissolvable (TDFe), labile particulate (LPFe) and total particulate (TPFe) iron in the Celtic Sea (NE Atlantic Ocean). Preferential uptake of SFe occurred during the spring bloom, preceding the removal of CFe. Uptake and export of Fe during the spring bloom, coupled with a reduction in vertical exchange, led to Fe deplete surface waters (<0.2 nM DFe; 0.11 nM LPFe, 0.45 nM TDFe, 1.84 nM TPFe) during summer stratification. Below the seasonal thermocline, DFe concentrations increased from spring to autumn, mirroring NO_3^- and consistent with supply from remineralised sinking organic material, and cycled independently of particulate Fe over seasonal timescales. These results demonstrate that summer Fe availability is comparable to the seasonally Fe limited Ross Sea shelf, and therefore is likely low enough to affect phytoplankton growth and species composition.

1. Introduction

Shelf seas cover <10% of the global ocean surface area, yet contribute 10-20% of global oceanic primary production [*Muller-Karger et al.*, 2005]. Iron is an essential element for phytoplankton growth and hence plays a pivotal role in the functioning of marine ecosystems and the ocean carbon cycle [*Boyd and Ellwood*, 2010; *Twining and Baines*, 2013]. Shelf seas are assumed to be Fe replete due to riverine and groundwater inputs, sediment resuspension and diagenetic supplies [e.g. *Chase et al.*, 2005; *Elrod et al.*, 2004; *Homoky et al.*, 2012; *Lohan and Bruland*, 2008; *Ussher et al.*, 2007]. However, seasonal Fe limitation has been demonstrated over narrow shelf regions of the Californian upwelling system [*Hutchins and Bruland*, 1998; *King and Barbeau*, 2007], in the Ross Sea [*Sedwick et al.*, 2011] and over the Bering Sea shelf break [*Aguilar-Islas et al.*, 2007]. Furthermore, the ability of an Atlantic coastal *Synechococcus* strain to alter its physiology in response to variable Fe availability [*Mackey et al.*, 2015], and expression of genes encoding flavodoxin in

coastal diatoms [*Chappell et al.*, 2015], emphasise the importance of understanding Fe availability to phytoplankton in dynamic shelf regions.

Evidence of Fe stress at elevated DFe concentrations (0.40-1.73 nM) [*Blain et al.*, 2004; *Chappell et al.*, 2015] highlights the need to consider not just DFe concentration, but also the physico-chemical speciation of Fe, which influences bioavailability [*Hassler and Schoemann*, 2009; *Hutchins et al.*, 1999; *Lis et al.*, 2015]. In shelf systems, particulate Fe dominates the total Fe inventory [*Hong and Kester*, 1986], where up to 81% can be in a labile particulate fraction [*Hurst et al.*, 2010]. This LPFe is considered available to phytoplankton, accessed directly from the particulate phase or indirectly following dissolution [*Chase et al.*, 2005; *Hurst et al.*, 2010; *Rubin et al.*, 2011]. Dissolved Fe can be further quantified in terms of SFe (<0.02 µm) and CFe (0.02-0.2 µm); with the CFe fraction found to comprise 60-80% of the DFe pool in continental shelf waters [*Hurst et al.*, 2010]. Dissimilar bioavailability of SFe and CFe has been demonstrated in laboratory studies [*Chen et al.*, 2003; *Chen and Wang*, 2001].

As part of the UK Shelf Sea Biogeochemistry programme (http://www.uk-ssb.org/), we investigated the cycling and distribution of the physico-chemical speciation of Fe in the central Celtic Sea. As a seasonally stratifying shelf sea, the degree of vertical mixing determines the availability of light and nutrients to phytoplankton [*Pingree et al.*, 1976]. To date, research into Celtic Sea nutrient cycling has predominantly focussed on the availability of NO_3^- to phytoplankton [*Hickman et al.*, 2012; *Pingree et al.*, 1976; *Sharples et al.*, 2001, 2009; *Williams et al.*, 2013], which is exhausted in surface waters following the onset of stratification and the phytoplankton spring bloom in April. Here we show that all potentially available Fe sources were also drawn down to limiting concentrations in the surface mixed layer (SML), implying that this system is likely limited by both Fe and NO_3^-.

2. Methods

Sampling was conducted during three cruises (November 2014, April 2015 and July 2015) on-board the *R.R.S. Discovery* at a central Celtic Sea station known as CCS (Fig. 1). Full details of methods are provided in the Supporting Information 1, and a glossary of the Fe fractions are presented in Table 1. Briefly, all trace metal samples were collected following GEOTRACES protocols [*Cutter et al.*, 2010]. Dissolved Fe (0.2 µm filtered), SFe (0.02 µm filtered) and TDFe (unfiltered) were analysed using flow injection with chemiluminesence detection [*Floor et al.*, 2015; *Obata et al.*, 1993], after spiking with hydrogen peroxide [*Lohan et al.*, 2006]. Colloidal Fe (0.02-0.2 µm) was determined by calculating the difference between the DFe and SFe concentrations. Particulate samples (≥0.45 µm) were collected on membrane filters and subjected to a sequential leach-digest procedure [*Milne et al.*, 2017]. The LPFe fraction was determined following protocols adapted from *Berger et al.* [2008] with 25% acetic acid as the leach reagent. For determination of total TPFe, a sequential acid digestion modified from *Ohnemus et al.* [2014] was used. All particulate digest samples were analysed using inductively coupled plasma-mass spectrometry.

Nitrate plus nitrite (hereafter NO_3^-) concentrations were measured at sea using segmented flow techniques with spectrophotometric detection [*Brewer and Riley*, 1965; *Woodward and Rees*, 2001] and International GO-SHIP sampling and handling protocols [*Hydes et al.*, 2010]. Salinity, temperature, and depth were measured using a CTD system (Seabird 911+), equipped with optical backscatter, dissolved oxygen (O_2) and chlorophyll-*a* (chl-*a*) sensors which were calibrated daily [*Carritt and Carpenter*, 1966; *Holm-Hansen et al.*, 1965] on board ship.

Large seawater volumes (60-100 L) for determining radium (Ra) isotopes were pooled from Niskin bottles, and Ra extracted by adsorption onto manganese-impregnated acrylic fiber [*Sun and Torgersen*, 1998]. Radium activities were analysed by Radium Delayed Coincidence Counting [*Annett et al.*, 2013; *Garcia-Solsona et al.*, 2008; *Moore*, 2008; *Moore and Arnold*, 1996] and corrected for supported activity from parent isotopes.

3. Results and discussion

The central Celtic Sea is characterised by weak residual currents [*Pingree and Le Cann*, 1989] with a water residence time of 1-2 years [*Bailly Du Bois et al.*, 2002]. Consequently, by sampling over autumn (November 2014), spring (April 2015) and summer (July 2015) we were able to capture the seasonality of these waters over a one year cycle.

3.1 Conditions following winter mixing

At the onset of seasonal stratification (3rd April, 2015), the vertical distributions of DFe (0.82 ± 0.041 nM, *n*=6) and NO_3^- (6.68 ± 0.370 µM, *n*=14) were relatively uniform, with only minor evidence of surface drawdown, and thus reflecting winter mixing conditions and concentrations before the spring bloom (Fig. 2a,b). In contrast, sediment resuspension increased the concentrations of TPFe and LPFe in near bottom samples (185.1 and 13.0 nM) relative to samples collected at 20 m (87.4 and 5.7 nM). At this time, CFe comprised 59-81% of DFe (Fig. 2e,f), similar to the contributions observed near the North West Atlantic continental margin [*Fitzsimmons et al.*, 2015a] and shelf regions of the Bering Sea [*Hurst et al.*, 2010], though less variable than in the Canary basin [*Ussher et al.*, 2010]. The CFe ratio was greater than the ~50:50 partitioning observed in deep oceanic waters [*Fitzsimmons et al.*, 2015a; *Ussher et al.*, 2010]. Therefore, this suggests either enhanced input of colloidal material from sediment resuspension and/or from break up of organic material, which particle reactive metals such as Fe associate with.

3.2 Iron and nitrate uptake during the spring phytoplankton bloom

During the phytoplankton spring bloom (3^{rd}-26^{th} April, 2015), both DFe and NO_3^- were removed from the SML, where a depletion of 4.93 µM of NO_3^- at 20 m was observed (Fig 2b,g), consistent with published NO_3^- data [*Fasham et al.*, 1983]. Here we observed a 0.53 nM depletion of DFe as part of the first seasonal Fe data set for this region (Fig. 2a,g). If all the DFe drawdown was a result of biological uptake this would equate to a phytoplankton Fe:N (nM:µM) ratio of 0.11, this calculation assumes no loss of DFe through scavenging and/or input via solubilisation of LPFe. Nevertheless, the uptake ratio calculated here is within the range reported for cultured phytoplankton grown in Fe replete environments [0.05-0.9 nM Fe: µM N; *Ho et al.*, 2003; *Sunda and Huntsman*, 1997], suggesting that phytoplankton species with a low to moderate Fe requirement would not have been affected by Fe stress during the spring bloom. . Moreover, the concentration of the LPFe fraction, which is considered a bioavailable source of Fe [*Chase et al.*, 2005; *Hurst et al.*, 2010; *Milne et al.*, 2017], was 3.96 ± 1.16 nM (*n*=4) at 20 m in April 2015 (Fig. 3c) and decreased by ~2 nM from 3^{rd}-16^{th} April 2015..

Distinct temporal trends in the different size fractions of DFe were observed during the spring bloom. At the start of the bloom (5^{th}-12^{th} April, 2015), SFe decreased from 0.33 ± 0.000 to 0.16 ± 0.007 nM (; Fig. 2g). In contrast, the CFe concentration remained constant at 0.42 ± 0.026 nM (3^{rd}-16^{th} April, 2015, *n=4;* Fig. 2g), suggesting that aggregation to the colloidal fraction was not a major removal pathway for sFe at this time, unless colloidal Fe was being removed at an equal rate to that of sFe aggregation. Therefore, these results suggest that phytoplankton preferentially utilized SFe during the initial stages of the bloom, consistent with laboratory culture studies [*Chen et al.*, 2003; *Chen and Wang*, 2001]. A decrease in CFe concentration from 0.40 ± 0.030 to 0.13 ± 0.010 nM (Fig. 2g) occurred once

the bloom had established (16^{th}-26^{th} April, 2015). Biological uptake of CFe by phytoplankton can occur, either directly [*Nodwell and Price*, 2001; *Rubin et al.*, 2011] or indirectly, following dissolution to the soluble phase by ligand/light interaction [*Borer et al.*, 2005; *Sulzberger et al.*, 1989] or grazing [*Schmidt et al.*, 2016]. Given the scarcity of SFe (<0.16 nM), and elevated primary production, at this time, it is probable that biological uptake contributed to the depletion of CFe in the SML. Preferential removal of SFe appears to contrast with observations in the open ocean, where preferential CFe uptake is hypothesised to be the cause of CFe minima in the deep chlorophyll maximum [*Fitzsimmons et al.*, 2015a]. Our spring bloom time-series in a shelf environment allows us to suggest that SFe is the more bioavailable fraction as SFe uptake precedes the removal of CFe, and therefore the observed CFe minima represents the net effect of SFe and CFe removal processes.

The observed timescale of CFe removal from the SML (~10 days), is consistent with the typically short residence times of colloidal thorium, which is in the order of hours to days in shelf waters [*Baskaran et al.*, 1992; *Moran and Buesseler*, 1993]. This suggests that the decreasing CFe concentration reflected a change in the balance between sources and sinks of colloids over these timescales. In addition to biological uptake, both adsorption and coagulation of CFe lead to particle formation [*Honeyman and Santschi*, 1991] and potential export from the SML. Using profiles of excess radium activity (Ra_{XS}) ($^{224}Ra_{XS}$ half-live= 3.66 days, $^{223}Ra_{XS}$ half-live= 11.4 days) as a tracer of vertical mixing (Fig. S1), we show that increasing stratification progressively restricted vertical exchange with CFe rich bottom waters, simultaneously reducing the supply of CFe to the SML.

3.3 Iron and nitrate availability during summer stratification

During summer stratification (July), the SML was depleted of both DFe (0.16 ± 0.071 nM, *n*= 15) and NO_3^- (typically <0.02 µM) (Table 1; Fig. 2a,b,c). As particulate Fe fractions were also quantified (Fig. 3a,b,c), we can consider all potentially bioavailable Fe sources. All

particulate Fe fractions were lowest in the SML during summer (Table 1), including LPFe which was 0.11 ± 0.003 nM. The removal of LPFe, as well as DFe, indicated that all potentially bioavailable Fe sources were depleted in the SML of the central Celtic Sea and raises the question of whether primary production in the SML was seasonally co-limited by Fe and NO_3^- availability.

Analogous Fe cycling occurs in seasonally Fe-limited shelf regions of the southern Ross Sea. In these waters, winter convective overturning supplies both DFe and particulate Fe to surface waters. Subsequent biological uptake and export coupled with a reduction in vertical exchange, leads to these waters becoming Fe limited in late spring/summer [*Marsay et al.*, 2014; *McGillicuddy et al.*, 2015; *Sedwick et al.*, 2011]. In contrast, the stratified central shelf waters of the Bering Sea maintain average summer SML LPFe concentrations of 6 nM, an important reservoir of bioavailable Fe for phytoplankton [*Hurst et al.*, 2010]. The central Celtic Sea represents an intermediate Fe cycle between these two environments. Unlike in the southern Ross Sea, complete NO_3^- drawdown is observed during summer (Fig. 2b), yet in this study the SML bioavailable Fe concentrations (DFe and LPFe; Figs. 2a, 3c) were similar, and much lower than observed in the central Bering Sea. We hypothesize that the Celtic Sea ecosystem exists in a fine balance of Fe and NO_3^- availability. Therefore, the structure of the summer ecosystem would be sensitive to changes in the availability of both nutrients. In the central Celtic Sea smaller species (< 20 μm) dominate the summer phytoplankton community, with *Synechococcus* most abundant [*Sharples et al.*, 2007]. Small phytoplankton have a competitive advantage over larger phytoplankton in Fe deplete waters [*Lis et al.*, 2015]. Moreover, *Synechococcus* species has been shown to dominate in Fe-limited Southern Californian stratified coastal waters, where upon the addition of Fe the ecosystem shifted in favour of diatom growth [*Hopkinson and Barbeau*, 2008].

The DFe pool in the SML during July 2015 represents the Fe maintained through efficient recycling in [*Strzepek et al.*, 2005] in these nutrient poor waters. On average, the concentration of SFe (0.13 ± 0.069 nM *n*=3) was in excess of the colloidal fraction (0.07 ± 0.092 nM, *n*=3) (Fig. 2e,f). Interestingly, these shelf concentrations were comparable to those seen in central oligotrophic gyres such as those observed at station ALOHA where SFe ranged from 0.05 - 0.1 nM in the upper 150 m, whereas CFe was depleted in the chlorophyll maximum [*Fitzsimmons et al.*, 2015b]. Although the concentration of SFe was low in both systems, it exceeded the solubility of the hydrolysis species [*Liu and Millero*, 2002]. Siderophores are low molecular weight complexes with high affinity and specificity for Fe(III) that are produced by marine bacterioplankton [*Gledhill et al.*, 2004], which may maintain the low, but persistent, SFe concentration in oligotrophic surface waters.

During summer months, the biomass maximum in the central Celtic Sea is observed below the SML, as a sub-surface chlorophyll maximum located in the pycnocline (Fig. 2c,d). This is an important region of new production as phytoplankton are able to access the diapycnal flux of nutrients from the bottom mixed layer (BML) [*Hickman et al.*, 2012]. Within the pycnocline, zonation of phytoplankton species is driven by vertical gradients in light and NO_3^- [*Hickman et al.*, 2009]. Here we observed a vertical gradient in DFe, NO_3^- (Fig. 2h) and photosynthetically available radiation of 16.4-0.11 W m^{-2} (during daytime casts). Photoacclimation at these light levels leads to increased cellular Fe quotas [*Strzepek and Price*, 2000; *Sunda and Huntsman*, 1997]. Where the flux of Fe across the pycnocline is insufficient to meet requirements, Fe and light co-limitation influences phytoplankton species composition in the sub-surface chlorophyll maximum [*Hopkinson and Barbeau*, 2008; *Johnson et al.*, 2010]. The nutrient concentrations observed in these studies (dFe 0.11-1.10 nM, NO_3^- 0.3-6.5 µM) were similar to those observed at the July SCM in the central Celtic Sea (dFe 0.09-0.93 nM, NO_3^- 0.02-7.61 µM), indicating the potential for Fe/light co-

limitation. However, an estimate of the diffusive flux of DFe and NO_3^- through the thermocline indicated a DFe:NO_3^- (nM: µM) ratio of new production of 0.19 (Supporting Information 3). This is similar to the uptake ratio (0.11) observed during the spring bloom, suggesting that the growth of phytoplankton species with a low to moderate Fe requirement would be supported by this flux, though importantly this assumes complete biological utilisation and no loss to scavenging. .

3.4 Iron and nitrate availability during the autumn phytoplankton bloom

Water column stratification was also observed in autumn (November) (Fig. 2c), and was reflected in the profiles of DFe, NO_3^- and all particulate Fe fractions (Fig. 2 a,b; Fig. 3a,b,c). Radium activity profiles also showed complete depletion in the SML in November 2014 (Fig. S1). The short half-lives of ^{223}Ra and ^{224}Ra indicate that rapid vertical exchange was still largely limited by the persistence of the seasonal pycnocline into November. Although still stratified, a net heat flux to the atmosphere meant stratification was progressively weakening relative to summer conditions [*Pingree et al.*, 1976] (Fig. 2c). The relative increase in vertical exchange resulted in higher SML concentrations of bioavailable Fe and NO_3^-, than observed during the summer stratified period (Table 1; Fig. 2a,b; Fig. 3c). The increased supply of nutrients (including Fe) fuelled an autumn bloom; observed here as elevated chl-*a* concentrations of ~ 0.7 mg m^{-3} (Fig. 2d).

3.5 Seasonal cycling in the bottom mixed layer

A seasonal build-up of DFe and NO_3^- in the BML (Fig. 2a,b) occurred alongside an increase in dissolved inorganic carbon (DIC) [*Humphreys.*, 2017] and a decrease in dissolved oxygen (O_2) (Spring ~284 µM, Summer ~261 µM, Autumn ~235 µM). The seasonal redistribution of NO_3^-, DIC and O_2 was consistent with previous findings suggesting NO_3^- cycling was driven by uptake in the SML and subsequent remineralisation in the BML [*Hickman et al.*, 2012; *Sharples et al.*, 2001]. When DFe concentrations from both the SML and BML (all seasons) are compared with corresponding NO_3^- concentrations a statistically

significant relationship is noted (r^2= 0.94, p< 0.001, *n*= 163; Fig. 3d), suggesting that similar processes drive the observed seasonality of DFe. Moreover, an estimated 95% of the organic carbon present in Celtic Sea surface sediments is remineralised in repeated resuspension cycles rather than preserved [*de Haas et al.*, 2002]. Our results suggest a similar process is occurring for the Fe associated with the organic matter. Additionally, no clear increase of DFe towards the seabed is observed in our profiles (Fig. 2a) to suggest a significant diffusive sedimentary input of DFe. This is in contrast to a localised area in the north-eastern Celtic Sea where weaker current and wave activity permit the deposition of fine, organic-rich sediment [*de Haas et al.*, 2002; *McCave*, 1971], and a significant benthic source of DFe to the overlying water column was observed at the time of our study [Fig.1; *Klar et al.*, 2017].

The majority (>99%) of DFe present in seawater is associated with organic complexes [*Gledhill and Buck*, 2012] which enhance the solubility of DFe in seawater above that of inorganic species [*Liu and Millero*, 2002]. Moreover, the concentration of organic-Fe chelators has been shown to control the solubility of Fe in particle rich coastal and shelf waters [*Buck and Bruland*, 2007; *Buck et al.*, 2007]; in the BML the LPFe fraction (Fig. 3c) was always in excess of DFe (Fig. 2a). Partial remineralisation of organic matter releases both DFe and organic Fe binding complexes [*Boyd et al.*, 2010], which provides a potential mechanism for the seasonal increase in DFe concentrations. Temperature and pH also affect the solubility of Fe in seawater [*Liu and Millero*, 2002] and the binding strength of organic Fe-binding complexes [*Avendaño et al.*, 2016; *Gledhill et al.*, 2015], and could account for the seasonal build-up of dFe in the BML. The seasonal changes of temperature and pH in the BML were ~2^{o}C and ~0.1 pH (*Humphreys.* [2017]) in the BML are thus considered insufficient to account for the seasonal build-up of DFe.

In contrast to DFe, the concentration of TDFe in the BML correlated with turbidity (Fig. 3e), indicating that short-term resuspension events were the primary cause of high

particulate Fe concentrations. Sediment resuspension events are driven by processes occurring on shorter timescales than seasonal changes (e.g. semi-diurnal tides, internal tides, and storm events) and result in high particle loads in the BML of shelf systems relative to open ocean waters. Furthermore, the observed TPFe:TPAl molar ratio was seasonally invariant and ranged from 0.22-0.28, similar to the upper crustal ratio [0.19-0.23; *McLennan*, 2001; *Rudnick and Gao*, 2003; *Wedepohl*, 1995], and consistent with the majority of TPFe being supplied from a lithogenic source. Our results indicate that a large proportion of particulate Fe (~80%) is refractory (Fig. 3b,c) and cycles independently of DFe. This is consistent with the majority of the Celtic Sea surface sediments being relict deposits from the Pleistocene and early Holocene, consisting of reworked, fine and coarse sands [*de Haas et al.*, 2002].

4. Conclusions

Our results show a seasonal, nutrient-type cycling of dFe in a temperate shelf sea. During summer, stratification isolates surface waters from Fe rich bottom waters and provides a mechanism whereby temperate and high latitude shelf sea ecosystems can become sensitive to Fe availability. The strength of seasonal stratification in North West European shelf seas is predicted to increase by ~20% by the end of the 21st century as a result of climate change [*Holt et al.*, 2010]. Under these conditions the magnitude of the diapycnal nutrient flux, including dFe, will decrease, exacerbating the summer oligotrophic conditions. When assessing the effect this will have upon shelf sea primary production we assert that it is necessary to consider the role of Fe as potentially co-limiting nutrient.

5. Acknowledgments

The authors would like to thank the captain and crew of the RSS Discovery. This project was funded by the UK Natural Environment Research Council (NE/L501840/1 (AB), NE/K001779/1 (ML, SU, AM, PW), NE/K002023/1 (WG, AA), NE/K001973/1 (EA, DR, MG), NE/K002058/1 (EMSW, CA)). The authors declare no competing financial interest. All data that supports the findings of this study have been submitted to the British Oceanography Data Centre.

References

Aguilar-Islas, A. M., M. P. Hurst, K. N. Buck, B. Sohst, G. J. Smith, M. C. Lohan, and K. W. Bruland (2007), Micro-and macronutrients in the southeastern Bering Sea: Insight into iron-replete and iron-depleted regimes, *Progress in Oceanography*, *73*(2), 99-126, doi:https://doi.org/10.1016/j.pocean.2006.12.002.

Annett, A. L., S. F. Henley, P. Van Beek, M. Souhaut, R. Ganeshram, H. J. Venables, M. P. Meredith, and W. Geibert (2013), Use of radium isotopes to estimate mixing rates and trace sediment inputs to surface waters in northern Marguerite Bay, Antarctic Peninsula, *Antarctic Science*, *25*(03), 445-456, doi:https://doi.org/10.1017/S0954102012000892.

Avendaño, L., M. Gledhill, E. P. Achterberg, V. M. C. Rérolle, and C. Schlosser (2016), Influence of ocean acidification on the organic complexation of iron and copper in Northwest European shelf seas; a combined observational and model study, *Frontiers in Marine Science*, *3*, doi:10.3389/fmars.2016.00058.

Bailly Du Bois, P., P. Germain, M. Rozet, and L. Solier (2002), Water masses circulation and residence time in the Celtic Sea and English Channel approaches, characterisation based on radionuclides labelling from industrial releases, in *International Conference on Radioactivity in Environment*, edited by P. Borretzen, T. Jolle and P. Strand, pp. 395-399, Monaco.

Baskaran, M., P. H. Santschi, G. Benoit, and B. Honeyman (1992), Scavenging of thorium isotopes by colloids in seawater of the Gulf of Mexico, *Geochimica et cosmochimica Acta*, *56*(9), 3375-3388, doi:https://doi.org/10.1016/0016-7037(92)90385-V.

Berger, C. J., S. M. Lippiatt, M. G. Lawrence, and K. W. Bruland (2008), Application of a chemical leach technique for estimating labile particulate aluminum, iron, and manganese in the Columbia River plume and coastal waters off Oregon and Washington, *Journal of Geophysical Research*, *113*(C2), doi:10.1029/2007JC004703.

Blain, S., C. Guieu, H. Claustre, K. Leblanc, T. Moutin, B. Quèguiner, J. Ras, and G. Sarthou (2004), Availability of iron and major nutrients for phytoplankton in the northeast Atlantic Ocean, *Limnology and Oceanography*, *49*(6), 2095-2104, doi:10.4319/lo.2004.49.6.2095.

Borer, P. M., B. Sulzberger, P. Reichard, and S. M. Kraemer (2005), Effect of siderophores on the light-induced dissolution of colloidal iron(III) (hydr)oxides, *Marine Chemistry*, *93*(2–4), 179-193, doi:http://dx.doi.org/10.1016/j.marchem.2004.08.006.

Boyd, P., E. Ibisanmi, S. Sander, K. Hunter, and G. Jackson (2010), Remineralization of upper ocean particles: Implications for iron biogeochemistry, *Limnology and Oceanography*, *55*(3), 1271, doi:10.4319/lo.2010.55.3.1271.
Boyd, P. W., and M. J. Ellwood (2010), The biogeochemical cycle of iron in the ocean, *Nature Geoscience*, *3*(10), 675-682, doi:doi:10.1038/ngeo964.
Brewer, P., and J. Riley (1965), The automatic determination of nitrate in sea water, paper presented at Deep Sea Research and Oceanographic Abstracts, Elsevier.
Buck, K. N., and K. W. Bruland (2007), The physicochemical speciation of dissolved iron in the Bering Sea, Alaska, *Limnology and Oceanography*, *52*(5), 1800, doi:10.4319/lo.2007.52.5.1800.
Buck, K. N., M. C. Lohan, C. J. Berger, and K. W. Bruland (2007), Dissolved iron speciation in two distinct river plumes and an estuary: Implications for riverine iron supply, *Limnology and Oceanography*, *52*(2), 843-855, doi:10.4319/lo.2007.52.2.0843.
Carritt, D., E, and J. Carpenter, H (1966), Comparison and evaluation of currently employed modifications of the Winkler method for determining dissolved oxygen in seawater; a NASCO report, *Journal of Marine Reseaidi*, *24*, 286-318.
Chappell, P. D., L. P. Whitney, J. R. Wallace, A. I. Darer, S. Jean-Charles, and B. D. Jenkins (2015), Genetic indicators of iron limitation in wild populations of Thalassiosira oceanica from the northeast Pacific Ocean, *ISME J*, *9*(3), 592-602, doi:10.1038/ismej.2014.171.
Chase, Z., B. Hales, T. Cowles, R. Schwartz, and A. van Geen (2005), Distribution and variability of iron input to Oregon coastal waters during the upwelling season, *Journal of Geophysical Research: Oceans*, *110*(C10), n/a-n/a, doi:10.1029/2004JC002590.
Chen, M., R. C. H. Dei, W.-X. Wang, and L. Guo (2003), Marine diatom uptake of iron bound with natural colloids of different origins, *Marine Chemistry*, *81*(3–4), 177-189, doi:http://dx.doi.org/10.1016/S0304-4203(03)00032-X.
Chen, M., and W.-X. Wang (2001), Bioavailability of natural colloid-bound iron to marine plankton: Influences of colloidal size and aging, *Limnology and oceanography*, *46*(8), 1956-1967.
Cutter, G., P. Andersson, L. Codispoti, P. Croot, R. Francois, M. Lohan, H. Obata, and M. Rutgers vd Loeff (2010), Sampling and sample-handling protocols for GEOTRACES Cruises, edited, doi:10013/epic.42722.
de Haas, H., T. C. E. van Weering, and H. de Stigter (2002), Organic carbon in shelf seas: sinks or sources, processes and products, *Continental Shelf Research*, *22*(5), 691-717, doi:http://dx.doi.org/10.1016/S0278-4343(01)00093-0.
Elrod, V. A., W. M. Berelson, K. H. Coale, and K. S. Johnson (2004), The flux of iron from continental shelf sediments: A missing source for global budgets, *Geophysical Research Letters*, *31*(12).
Fasham, M. J. R., P. M. Holligan, and P. R. Pugh (1983), The spatial and temporal development of the spring phytoplankton bloom in the Celtic Sea, April 1979, *Progress in Oceanography*, *12*(1), 87-145, doi:http://dx.doi.org/10.1016/0079-6611(83)90007-1.
Fitzsimmons, J. N., G. G. Carrasco, J. Wu, S. Roshan, M. Hatta, C. I. Measures, T. M. Conway, S. G. John, and E. A. Boyle (2015a), Partitioning of dissolved iron and iron isotopes into soluble and colloidal phases along the GA03 GEOTRACES North Atlantic Transect, *Deep Sea Research Part II: Topical Studies in Oceanography*, *116*, 130-151, doi:http://dx.doi.org/10.1016/j.dsr2.2014.11.014.

Fitzsimmons, J. N., C. T. Hayes, S. N. Al-Subiai, R. Zhang, P. L. Morton, R. E. Weisend, F. Ascani, and E. A. Boyle (2015b), Daily to decadal variability of size-fractionated iron and iron-binding ligands at the Hawaii Ocean Time-series Station ALOHA, *Geochimica et Cosmochimica Acta*, *171*, 303-324.
Floor, G. H., R. Clough, M. C. Lohan, S. J. Ussher, P. J. Worsfold, and C. R. Quétel (2015), Combined uncertainty estimation for the determination of the dissolved iron amount content in seawater using flow injection with chemiluminescence detection, *Limnology and Oceanography: Methods*, *13*(12), 673-686, doi:10.1002/lom3.10057.

Garcia-Solsona, E., J. Garcia-Orellana, P. Masqué, and H. Dulaiova (2008), Uncertainties associated with ^{223}Ra and ^{224}Ra measurements in water via a Delayed Coincidence Counter (RaDeCC), *Marine Chemistry*, *109*(3), 198-219.
Gledhill, M., E. P. Achterberg, K. Li, K. N. Mohamed, and M. J. Rijkenberg (2015), Influence of ocean acidification on the complexation of iron and copper by organic ligands in estuarine waters, *Marine Chemistry*, *177*, 421-433.
Gledhill, M., and K. N. Buck (2012), The organic complexation of iron in the marine environment: a review, *Frontiers in microbiology*, *3*, doi:10.3389/fmicb.2012.00069.
Gledhill, M., P. McCormack, S. Ussher, E. P. Achterberg, R. F. C. Mantoura, and P. J. Worsfold (2004), Production of siderophore type chelates by mixed bacterioplankton populations in nutrient enriched seawater incubations, *Marine Chemistry*, *88*(1), 75-83.
Hassler, C., and V. Schoemann (2009), Bioavailability of organically bound Fe to model phytoplankton of the Southern Ocean, *Biogeosciences*, *6*(10), 2281-2296.
Hickman, A. E., P. M. Holligan, C. M. Moore, J. Sharples, V. Krivtsov, and M. R. Palmer (2009), Distribution and chromatic adaptation of phytoplankton within a shelf sea thermocline, *Limnology and Oceanography*, *54*(2), 525-536, doi:10.4319/lo.2009.54.2.0525.
Hickman, A. E., C. M. Moore, J. Sharples, M. I. Lucas, G. H. Tilstone, V. Krivtsov, and P. M. Holligan (2012), Primary production and nitrate uptake within the seasonal thermocline of a stratified shelf sea, *Marine Ecology Progress Series*, *463*, 39-57.
Ho, T. Y., A. Quigg, Z. V. Finkel, A. J. Milligan, K. Wyman, P. G. Falkowski, and F. M. Morel (2003), The elemental composition of some marine phytoplankton, *Journal of Phycology*, *39*(6), 1145-1159.
Holm-Hansen, O., C. J. Lorenzen, R. W. Holmes, and J. D. Strickland (1965), Fluorometric determination of chlorophyll, *Journal du Conseil*, *30*(1), 3-15.
Holt, J., S. Wakelin, J. Lowe, and J. Tinker (2010), The potential impacts of climate change on the hydrography of the northwest European continental shelf, *Progress in Oceanography*, *86*(3–4), 361-379, doi:http://doi.org/10.1016/j.pocean.2010.05.003.
Homoky, W. B., S. Severmann, J. McManus, W. M. Berelson, T. E. Riedel, P. J. Statham, and R. A. Mills (2012), Dissolved oxygen and suspended particles regulate the benthic flux of iron from continental margins, *Marine Chemistry*, *134*, 59-70.
Honeyman, B. D., and P. H. Santschi (1991), Coupling adsorption and particle aggregation: laboratory studies of" colloidal pumping" using iron-59-labeled hematite, *Environmental science & technology*, *25*(10), 1739-1747.
Hong, H., and D. R. Kester (1986), Redox state of iron in the offshore waters of Peru, *Limnol. Oceanogr*, *31*(3), 512-524.
Hopkinson, B. M., and K. A. Barbeau (2008), Interactive influences of iron and light limitation on phytoplankton at subsurface chlorophyll maxima in the eastern North Pacific, *Limnology and Oceanography*, *53*(4), 1303-1318, doi:10.4319/lo.2008.53.4.1303.
Humphreys., M. P. (2017), Mechanisms for a nutrient-conserving carbon pump in a seasonally stratified, temperate continental shelf sea. (pers comm)
Hurst, M. P., A. M. Aguilar-Islas, and K. W. Bruland (2010), Iron in the southeastern Bering Sea: elevated leachable particulate Fe in shelf bottom waters as an important source for surface waters, *Continental Shelf Research*, *30*(5), 467-480.
Hutchins, D. A., and K. W. Bruland (1998), Iron-limited diatom growth and Si:N uptake ratios in a coastal upwelling regime, *Nature*, *393*(6685), 561-564.
Hutchins, D. A., A. E. Witter, A. Butler, and G. W. Luther (1999), Competition among marine phytoplankton for different chelated iron species, *Nature*, *400*(6747), 858-861.
Hydes, D., M. Aoyama, A. Aminot, K. Bakker, S. Becker, S. Coverly, A. Daniel, A. Dickson, O. Grosso, and R. Kerouel (2010), Determination of dissolved nutrients (N, P, Si) in seawater with high precision and inter-comparability using gas-segmented continuous flow analysers, *The GO-SHIP Repeat Hydrography Manual: a collection of expert reports and guidelines; IOCCP report No.14, ICPO publication series No. 134, version 1*.

Johnson, Z. I., R. Shyam, A. E. Ritchie, C. Mioni, V. P. Lance, J. W. Murray, and E. R. Zinser (2010), The effect of iron-and light-limitation on phytoplankton communities of deep chlorophyll maxima of the western Pacific Ocean, *Journal of Marine Research*, *68*(2), 283-308.

King, A. L., and K. Barbeau (2007), Evidence for phytoplankton iron limitation in the southern California Current System, *Marine Ecology Progress Series*, *342*, 91-103.

Klar, J., W. B. Homoky, P. J. Statham, A. J. Birchill, E. Harris, E. M. S. Woodward, B. Silburn, M. Cooper, R. H. James, and D. P. Connelly (2017), Stability of dissolved and soluble Fe (II) in shelf sediment pore waters and release to an oxic water column, *Biogeochemistry*, doi:10.1007/s10533-017-0309-x.

Lis, H., Y. Shaked, C. Kranzler, N. Keren, and F. M. M. Morel (2015), Iron bioavailability to phytoplankton: an empirical approach, *ISME J*, *9*(4), 1003-1013, doi:10.1038/ismej.2014.199.

Liu, X., and F. J. Millero (2002), The solubility of iron in seawater, *Marine Chemistry*, *77*(1), 43-54.

Lohan, M. C., A. M. Aguilar-Islas, and K. W. Bruland (2006), Direct determination of iron in acidified (pH 1.7) seawater samples by flow injection analysis with catalytic spectrophotometric detection: Application and intercomparison, *Limnology and Oceanography: Methods*, *4*(6), 164-171, doi:10.4319/lom.2006.4.164.

Lohan, M. C., and K. W. Bruland (2008), Elevated Fe (II) and dissolved Fe in hypoxic shelf waters off Oregon and Washington: An enhanced source of iron to coastal upwelling regimes, *Environmental science & technology*, *42*(17), 6462-6468.

Mackey, K. R., A. F. Post, M. R. McIlvin, G. A. Cutter, S. G. John, and M. A. Saito (2015), Divergent responses of Atlantic coastal and oceanic Synechococcus to iron limitation, *Proceedings of the National Academy of Sciences*, *112*(32), 9944-9949.

Marsay, C. M., P. N. Sedwick, M. S. Dinniman, P. M. Barrett, S. L. Mack, and D. J. McGillicuddy (2014), Estimating the benthic efflux of dissolved iron on the Ross Sea continental shelf, *Geophysical Research Letters*, *41*(21), 7576-7583, doi:10.1002/2014GL061684.

McCave, I. N. (1971), Wave effectiveness at the sea bed and its relationship to bed-forms and deposition of mud, *Journal of Sedimentary Research*, *41*(1), 89-96, doi:10.1306/74d721f3-2b21-11d7-8648000102c1865d.

McGillicuddy, D. J., P. N. Sedwick, M. Dinniman, K. R. Arrigo, T. S. Bibby, B. J. Greenan, E. E. Hofmann, J. M. Klinck, W. O. Smith, and S. Mack (2015), Iron supply and demand in an Antarctic shelf ecosystem, *Geophysical Research Letters*, *42*(19), 8088-8097.

McLennan, S. M. (2001), Relationships between the trace element composition of sedimentary rocks and upper continental crust, *Geochemistry, Geophysics, Geosystems*, *2*(4).

Milne, A., C. Schlosser, B. D. Wake, E. P. Achterberg, R. Chance, A. Baker, A. Forryan, and M. C. Lohan (2017), Particulate phases are key in controlling dissolved iron concentrations in the (sub)-tropical North Atlantic, *Geophysical Research Letters*, *44*(5), 2377-2387, doi:10.1002/2016GL072314.

Moore, W. S. (2008), Fifteen years experience in measuring ^{224}Ra and ^{223}Ra by delayed-coincidence counting, *Marine Chemistry*, *109*(3), 188-197.

Moore, W. S., and R. Arnold (1996), Measurement of ^{223}Ra and ^{224}Ra in coastal waters using a delayed coincidence counter, *J. Geophys. Res*, *101*(C1), 1321-1329.

Moran, B. S., and K. O. Buesseler (1993), Size-fractionated ^{234}Th in continental shelf waters off New England: Implications for the role of colloids in oceanic trace metal scavenging, *Journal of Marine Research*, *51*(4), 893-922.

Muller-Karger, F. E., R. Varela, R. Thunell, R. Luerssen, C. Hu, and J. J. Walsh (2005), The importance of continental margins in the global carbon cycle, *Geophysical Research Letters*, *32*(1), doi:10.1029/2004GL021346.

National Geophysical Data Center, N. N. U. S. D. o. C. (1995), TerrainBase, Global 5 Arc-minute Ocean Depth and Land Elevation from the US National Geophysical Data Center (NGDC), edited, Research Data Archive at the National Center for Atmospheric Research, Computational and Information Systems Laboratory, Boulder, CO.

Nodwell, L. M., and N. M. Price (2001), Direct use of inorganic colloidal iron by marine mixotrophic phytoplankton, *Limnology and Oceanography*, *46*(4), 765-777, doi:10.4319/lo.2001.46.4.0765.

Obata, H., H. Karatani, and E. Nakayama (1993), Automated determination of iron in seawater by chelating resin concentration and chemiluminescence detection, *Analytical Chemistry*, *65*(11), 1524-1528, doi:10.1021/ac00059a007.
Ohnemus, D. C., M. E. Auro, R. M. Sherrell, M. Lagerstrom, P. L. Morton, B. S. Twining, S. Rauschenberg, and P. J. Lam (2014), Laboratory intercomparison of marine particulate digestions including Piranha: a novel chemical method for dissolution of polyethersulfone filters, *Limnol. Oceanogr.: Methods*, *12*, 530-547.
Pingree, R., P. Holligan, G. Mardell, and R. Head (1976), The influence of physical stability on spring, summer and autumn phytoplankton blooms in the Celtic Sea, *Journal of the Marine Biological Association of the United Kingdom*, *56*(04), 845-873.
Pingree, R. D., and B. Le Cann (1989), Celtic and Armorican slope and shelf residual currents, *Progress in Oceanography*, *23*(4), 303-338, doi:http://dx.doi.org/10.1016/0079-6611(89)90003-7.

Rubin, M., I. Berman-Frank, and Y. Shaked (2011), Dust-and mineral-iron utilization by the marine dinitrogen-fixer Trichodesmium, *Nature Geoscience*, *4*(8), 529-534.
Rudnick, R. L., and S. Gao (2003), 3.01 - Composition of the Continental Crust A2 - Holland, Heinrich D, in *Treatise on Geochemistry*, edited by K. K. Turekian, pp. 1-64, Pergamon, Oxford, doi:http://dx.doi.org/10.1016/B0-08-043751-6/03016-4.
Schmidt, K., C. Schlosser, A. Atkinson, S. Fielding, H. J. Venables, C. M. Waluda, and E. P. Achterberg (2016), Zooplankton gut passage mobilizes lithogenic iron for ocean productivity, *Current Biology*, *26*(19), 2667-2673.
Sedwick, P. N., C. M. Marsay, B. M. Sohst, A. M. Aguilar Islas, M. Lohan, M. C. Long, K. R. Arrigo, R. B. Dunbar, M. A. Saito, and W. O. Smith (2011), Early season depletion of dissolved iron in the Ross Sea polynya: Implications for iron dynamics on the Antarctic continental shelf, *Journal of Geophysical Research: Oceans*, *116*(19), doi: 10.1029/2010jc006553.
Sharples, J., C. M. Moore, A. E. Hickman, P. M. Holligan, J. F. Tweddle, M. R. Palmer, and J. H. Simpson (2009), Internal tidal mixing as a control on continental margin ecosystems, *Geophysical Research Letters*, *36*(23), doi:10.1029/2009GL040683.
Sharples, J., M. C. Moore, T. P. Rippeth, P. M. Holligan, D. J. Hydes, N. R. Fisher, and J. H. Simpson (2001), Phytoplankton distribution and survival in the thermocline, *Limnology and Oceanography*, *46*(3), 486-496.
Sharples, J., J. F. Tweddle, J. Mattias Green, M. R. Palmer, Y.-N. Kim, A. E. Hickman, P. M. Holligan, C. Moore, T. P. Rippeth, and J. H. Simpson (2007), Spring-neap modulation of internal tide mixing and vertical nitrate fluxes at a shelf edge in summer, *Limnology and Oceanography*, *52*(5), 1735-1747.

Strzepek, R., M. Maldonado, J. Higgins, J. Hall, K. Safi, S. Wilhelm, and P. Boyd (2005), Spinning the "Ferrous Wheel": The importance of the microbial community in an iron budget during the FeCycle experiment, *Global biogeochemical cycles*, *19*(4), doi:10.1029/2005GB002490.
Strzepek, R., and N. Price (2000), Influence of irradiance and temperature on the iron content of the marine diatom Thalassiosira weissflogii (Bacillariophyceae), *Marine Ecology Progress Series*, *206*, 107-117.
Sulzberger, B., D. Suter, C. Siffert, S. Banwart, and W. Stumm (1989), Dissolution of fe(III)(hydr)oxides in natural waters; laboratory assessment on the kinetics controlled by surface coordination, *Marine Chemistry*, *28*(1), 127-144, doi:http://dx.doi.org/10.1016/0304-4203(89)90191-6.
Sun, Y., and T. Torgersen (1998), The effects of water content and Mn-fiber surface conditions on ^{224}Ra measurement by ^{220}Rn emanation, *Marine Chemistry*, *62*(3), 299-306.
Sunda, W. G., and S. A. Huntsman (1997), Interrelated influence of iron, light and cell size on marine phytoplankton growth, *Nature*, *390*(6658), 389-392.
Twining, B. S., and S. B. Baines (2013), The trace metal composition of marine phytoplankton, *Annual review of marine science*, *5*, 191-215.

Ussher, S. J., E. P. Achterberg, G. Sarthou, P. Laan, H. J. W. de Baar, and P. J. Worsfold (2010), Distribution of size fractionated dissolved iron in the Canary Basin, *Marine Environmental Research*, *70*(1), 46-55, doi:http://dx.doi.org/10.1016/j.marenvres.2010.03.001.
Ussher, S. J., P. J. Worsfold, E. P. Achterberg, A. Laës, S. Blain, P. Laan, and H. J. De Baar (2007), Distribution and redox speciation of dissolved iron on the European continental margin, *Limnology and Oceanography: Methods*, *52*(6), 2530-2539.
Wedepohl, H. K. (1995), The composition of the continental crust, *Geochimica et Cosmochimica Acta*, *59*(7), 1217-1232.
Williams, C., J. Sharples, C. Mahaffey, and T. Rippeth (2013), Wind driven nutrient pulses to the subsurface chlorophyll maximum in seasonally stratified shelf seas, *Geophysical Research Letters*, *40*(20), 5467-5472.
Woodward, E., and A. Rees (2001), Nutrient distributions in an anticyclonic eddy in the northeast Atlantic Ocean, with reference to nanomolar ammonium concentrations, *Deep Sea Research Part II: Topical Studies in Oceanography*, *48*(4), 775-793.

Table 1- A glossary of the operationally defined iron fractions determined during this study. Full details are provided in Supporting Information 1. Concentrations of each fraction observed in surface waters are also displayed. For April 2015 the range of concentrations observed at 20 m are presented. For July 2015 the state of water column stratification was consistent and so the surface mixed layer was defined following *Hickman et al.* [2012]. In November 2014 the strength of stratification was variable and the surface mixed layer was determined by visual inspection of the profile.Fraction

	Abbreviation	**Filtration**	**Iron accessed**
Dissolved Iron	DFe	<0.2 µm	Includes all iron passing through 0.2 µm filter that is dissolved after a minimum of 2 months at pH 1.6. This includes both soluble and colloidal phases (see below).
Soluble Iron	SFe	<0.02 µm	Includes all iron passing through 0.02 µm filter that is dissolved after a minimum of 2 months at pH 1.6. This includes free inorganic species and iron bound to low molecular weight organic complexes.
Colloidal Iron	CFe	dFe-sFe	Includes Fe in the size fraction 0.02-0.2 µm. Includes iron containing nanoparticles and iron bound to organic material in the colloidal phase e.g. humic substances and polysaccharides.
Total Dissolvable Iron	TDFe	Unfiltered	Includes all iron dissolved from an unfiltered sample after a minimum of 6 months at pH 1.6. In this study concentrations were in excess of the sum of DFe and leachable particulate iron (see below), indicating that this treatment accessed refractory phases of particulate iron.
Leachable Particulate Iron	LPFe	>0.45 µm	Includes readily reducible iron oxyhydroxides and intracellular iron retained on a 0.45 µm filter.
Total Particulate Iron	TPFe	>0.45 µm	Includes all iron phases (refractory + leachable particulate iron) retained on a 0.45 µm filter.

	DFe (nM)	**SFe (nM)**	**CFe (nM)**	**TDFe (nM)**	**LPFe (nM)**	**TPFe (nM)**	**NO_3^- (µM)**
3rd- 26th April 2015	0.23 ± 0.002 to 0.76 ± 0.009	0.11 ± 0.010 to 0.33 ± 0.000	0.13 ± 0.010 to 0.43 ± 0.010	6.84 ± 0.085* to 46.81 ± 1.267	3.47 ± 0.07* to 5.69 ± 0.04	44.82± 0.22* to 87.37 ± 0.90	1.15 to 6.03
14-31st July 2015	0.16 ± 0.071 (*n*= 15)	0.13 ± 0.069 (*n*=3)	0.07 ± 0.092 (*n*=3)	0.45 ± 0.179 (*n*=14)	0.11 ± 0.003 (*n*=1)	1.84 ± 0.010 (*n*=1)	< 0.02 µM
11th-29th November 2014	0.29 ± 0.068 (*n*= 9)	0.14 ± 0.082 (*n*=3)	0.17 ± 0.036 (*n*=3)	3.73 ± 0.583 (*n*= 6)	0.34 ± 0.024 (*n*= 2)	4.26 ± 0.251 (*n*= 2)	2.33 ± 0.037 (*n*=14)

*TDFe samples collected 12-26th April, LPFe and TPFe samples collected from 3rd to 16th April

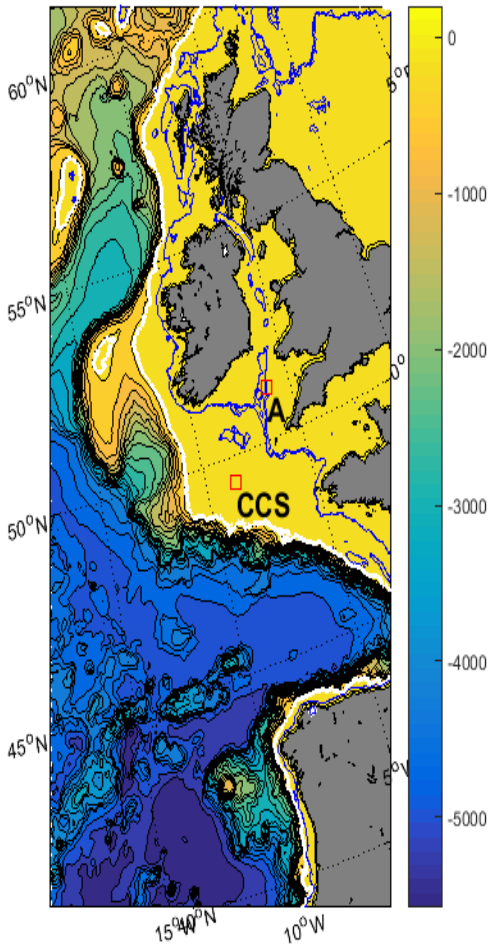

Figure 1- Map of Celtic Sea bathymetry (colour bar, m), the white line is the 200 m isobath and blue line is the 100 m isobath, data provided by the *National Geophysical Data Center* [1995]. The central Celtic Sea (CCS) sampling site (49° 24’ N, 8° 36’ W), ~150 m depth, was the location of this study. Site A (51° 12’ N, 6° 8’ W), ~100 m depth, was the primary sampling site of the study conducted by *Klar et al.* [2017].

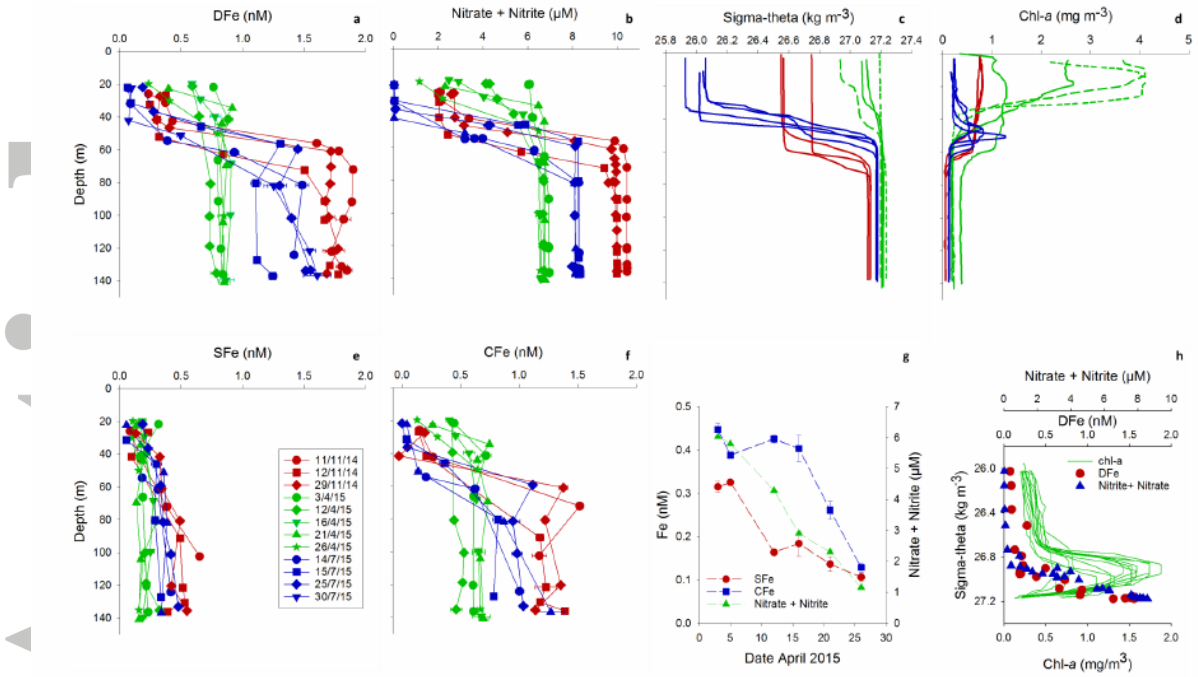

Figure 2- The seasonal time series of dFe at the Central Celtic Sea (CCS), November 2014 to July 2015. Top row relates DFe (a) to the oceanographic setting at the time of sampling, including the concentration of NO_3^- (limit of detection 0.02 µM) (b), the state of stratification (c), indicated by sigma-theta, and biomass (d), indicated by the chlorophyll-a concentration. Sigma-theta plots are identified by the month of sampling only (red= November 14', green= April 15', blue= July 15'), except the short dashed green line which represents the 3.4.15, from which point the surface density continuously decreased throughout April to the 26.4.15, represented by the large dashed green line. Chlorophyll-*a* plots are identified by month of sampling (same colour scheme as sigma-theta) except peak spring bloom chl-*a* concentrations on 16.4.15 (short dashed line) and 21.4.15 (long dashed line). The bottom row includes the temporal evolution of SFe (e) and CFe (f), which together make up DFe, shows the drawdown of SFe, CFe and NO_3^- at 20 m depth during the spring bloom in April 2015 (g) and the concentration of DFe and NO_3^- in the pycnocline during July 2015 (h), in relation to the subsurface chlorophyll-*a* maximum. The pycnocline region determined following *Hickman et al.* [2012]. Note that in July 2015, samples were collected for the determination of DFe during 14 casts', for clarity only those with corresponding SFe concentrations are displayed. For the full range of DFe concentrations see figure 3d.

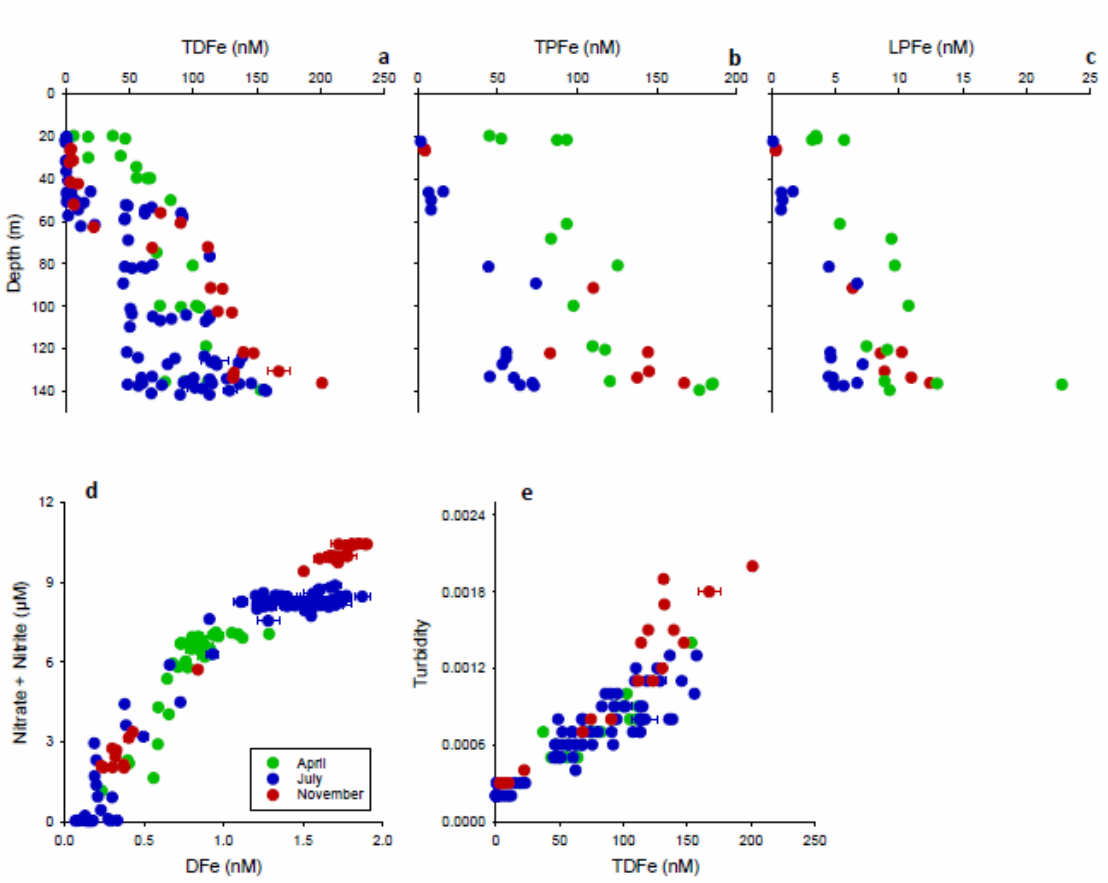

Figure 3- The seasonal time series of particulate iron in the central Celtic Sea, November 2014 to July 2015. Depth profiles of TDFe (a), PFe (b), LpFe (c). Bottom row displays close coupling between DFe and NO_3^- (d) (r^2=0.94) compared to the coupling between TDFe and particle load, as indicated by turbidity (e) (April r^2= 0.87, July r^2= 0.86 and November r^2=0.92).